Heliyon 9 (2023) e15698

Contents lists available at ScienceDirect

Heliyon

journal homepage: www.cell.com/heliyon

Research article

Acid-treated pomegranate peel; An efficient biosorbent for the excision of hexavalent chromium from wastewater

Rajan Rai [a], Ram Lochan Aryal [b], Hari Paudyal [c], Surendra Kumar Gautam [a], Kedar Nath Ghimire [c], Megh Raj Pokhrel [c], Bhoj Raj Poudel [a,c,*]

[a] Department of Chemistry, Tri-Chandra Multiple Campus, Tribhuvan University, Kathmandu, Nepal
[b] Department of Chemistry, Amrit Campus, Tribhuvan University, Kathmandu, Nepal
[c] Central Department of Chemistry, Tribhuvan University, Kirtipur, Kathmandu, Nepal

ARTICLE INFO

Keywords:
Biosorption
Cr(VI)
Human health
Isotherm
Wastewater treatment

ABSTRACT

We studied the sequestration of hexavalent chromium Cr(VI) from an aqueous solution using chemically modified pomegranate peel (CPP) as an efficient bio-adsorbent. The synthesized material was characterized by X-ray diffraction spectroscopy (XRD), Fourier-transform infrared spectroscopy (FTIR), energy dispersive spectroscopy (EDS), and scanning electron microscopy (SEM). The impacts of parameters like solution pH, Cr(VI) concentration, contact time, and adsorbent dosage were investigated. Experimental results of the isotherm studies and adsorption kinetics were found agreeing to the Langmuir isotherm model and pseudo-second-order kinetics, respectively. The CPP showed appreciable Cr(VI) remediation capacity with a maximal loading capacity of 82.99 mg/g at pH 2.0, which was obtained in 180 min at room temperature. Thermodynamic studies revealed the biosorption process as spontaneous, feasible, and thermodynamically favorable. The spent adsorbent was eventually regenerated and reused, and the safe disposal of Cr(VI) was ensured. The study revealed that the CPP can be effectively employed as an affordable sorbent for the excision of Cr(VI) from water.

1. Introduction

The mixing of micro-pollutants causes water to be detrimental to consumers. About 70% of illness, particularly in women and children has been confirmed to be related to water contamination in developing countries like Nepal [1]. Industrialization has always been contributing to the development of mankind, parallelly creating a global threat by the excessive release of heavy metals into the aquatic environment. Industrial wastewaters are found to possess various toxic metals like Arsenic (As), Cadmium (Cd), Chromium (Cr), Iron (Fe), Lead (Pb), Mercury (Hg), Nickel (Ni), and others. Heavy metals are non-biodegradable, and they can easily be accumulated in living tissues in an appreciable amount, which causes a significant threat to public health. Their effects include reduced growth and development, organ and nervous system damage, cancer, and even death [2,3]. These metals are introduced to the water by industrial activities like mining, metal plating, smelting, leather tanning, dyeing, pigment manufacture, battery manufacture, pesticides and fertilizer, and photography industries [4,5].

Chromium comes in contact with drinking water resources naturally through geochemical activity, soil and rock erosion, or anthropogenically by contamination from industrial sources such as tanneries, electroplating, alloying, textile processing, dying,

* Corresponding author. Department of Chemistry, Tri-Chandra Multiple Campus, Tribhuvan University, Kathmandu, Nepal.
E-mail address: chembrpoudel@gmail.com (B.R. Poudel).

https://doi.org/10.1016/j.heliyon.2023.e15698
Received 31 December 2022; Received in revised form 18 April 2023; Accepted 19 April 2023
Available online 24 April 2023

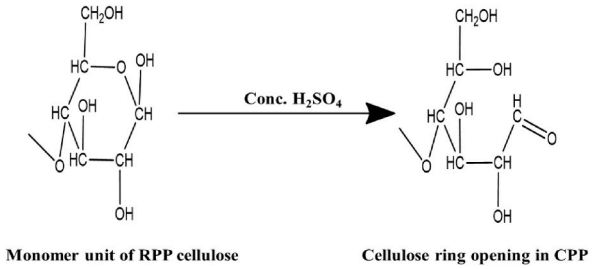

Scheme 1. Charring mechanism of RPP [33].

fertilizers, and pesticide production. It can exist in nine different oxidation states, among which the hexavalent and trivalent states are the most common [6]. Cr(VI) is highly toxic because it is highly soluble in water and can also be easily reduced [7,8]. This causes toxicity in living beings as it oxidizes some protein molecules and the DNA building block in humans [9], hence classified as the class 'A' human mutagen, carcinogen, and teratogen [10–13]. Cr(VI) concentrates in the food chain and causes several disorders in our health, including vomiting, diarrhea, hemorrhage, stomach ulcer, liver and kidney damage, and cancer [14–16]. Based on its fatal effects on human health, the WHO proclaimed that the maximum concentration of hexavalent chromium in drinking water should not be higher than 0.05 μg/L [17]. Its high rate of dispersion in the wide pH range of the aqueous phase, non-biodegradability, and toxic nature makes its removal from the natural environment necessary.

Several methods are being studied and used to eliminate Cr(VI) from the aquatic environment, some of which are ion exchange [18,19], electro-dialysis [20], redox reaction, membrane technology [21], and adsorption [22–24]. Most of the aforementioned solutions can only be used to a certain extent due to the requirement for expensive equipment, incomplete metal removal, hazardous waste sludge, and disposal [16,25–27]. According to reports, the adsorptive method of removal is the one most frequently utilized to remove Cr(VI) and other heavy metal contaminants from wastewater. The availability of less expensive materials for the manufacturing of affordable adsorbents is what has made this technique so popular [28,29]. This approach is more effective since even very low metal concentrations can be eliminated via biosorption. Agricultural by-products are found to possess ion exchange and adsorptive capacities due to the abundance of various functional groups in them. They can be employed as effective adsorbents in natural as well as modified forms.

Pomegranate, reported to be originated from Iran, is mainly cultivated in countries like Iran, Afghanistan, India, China, Saudi Arabia, America, Palestine, Africa, and Italy. It is one of the emerging fruit crops in Nepal [30]. Peels of this fruit are found to be rich in various functional groups such as carboxylic and hydroxyl groups [31]. After consumption of the fruit, the two-layered peel is discarded as degradable waste. In the current study, pomegranate peel powder was treated with H_2SO_4 to create a biomass-based adsorbent that was used to remove hexavalent chromium from water. Additionally, desorption of the metal ion was performed to investigate the possibility of recovering the adsorbed Cr(VI). We investigated the creation of inexpensive biosorbents using pomegranate peel as financial appropriateness is required for the absorption of chromium from water in rural areas since there is a lack of sufficient cheap material for the removal of Cr(VI) ions. The pomegranate peel is an excellent choice for us since it is often available as bio-waste in many locations, includes a variety of surface functional groups, and does not release soluble contaminants into the treated water. Additionally, acid modification may promote Cr(VI) ion adsorption because the acid treatment of pomegranate peel may offer a higher number of active sites that can interact chemically with Cr(VI), thereby improving chemisorption. As far as we are aware, no research has been done on the adsorption of Cr(VI) utilizing CPP as an adsorbent and subsequent regeneration of the metal ion. To remove Cr(VI) from the aqueous environment, CPP is therefore suggested as a new adsorbent. The goal of the current study was to examine the use of an accessible and widely available agricultural waste made from pomegranate peels that have undergone acid modification to remove hexavalent chromium from water. The prepared material was characterized by various techniques, namely EDS, XRD, SEM, and FTIR. Batch experiments were used to investigate the removal effectiveness of the adsorbent and the impact of experimental parameters on Cr(VI) adsorption.

2. Experimental

2.1. Preparation of solution

To make a stock solution of Cr(VI) (1000 mg/L), crystals of potassium dichromate were dissolved in distilled water. The dilution procedure was used to create working solutions from the stock solution at the required concentrations. 0.1 M HCl and 0.1 M NaCl solutions were used to adjust the desired initial pH value of the solution.

2.2. Preparation of the adsorbent

The pomegranate peels were collected from juice vendors around Kathmandu, Nepal. The tougher outer layer of the peel was washed with distilled water, dried in daylight for 15 days, and then oven-dried for 12 h at 80 °C. It was then ground into a fine powder and sieved to produce particles not larger than 220 μm in size. The pulverized pomegranate peel was considered raw adsorbent (RPP).

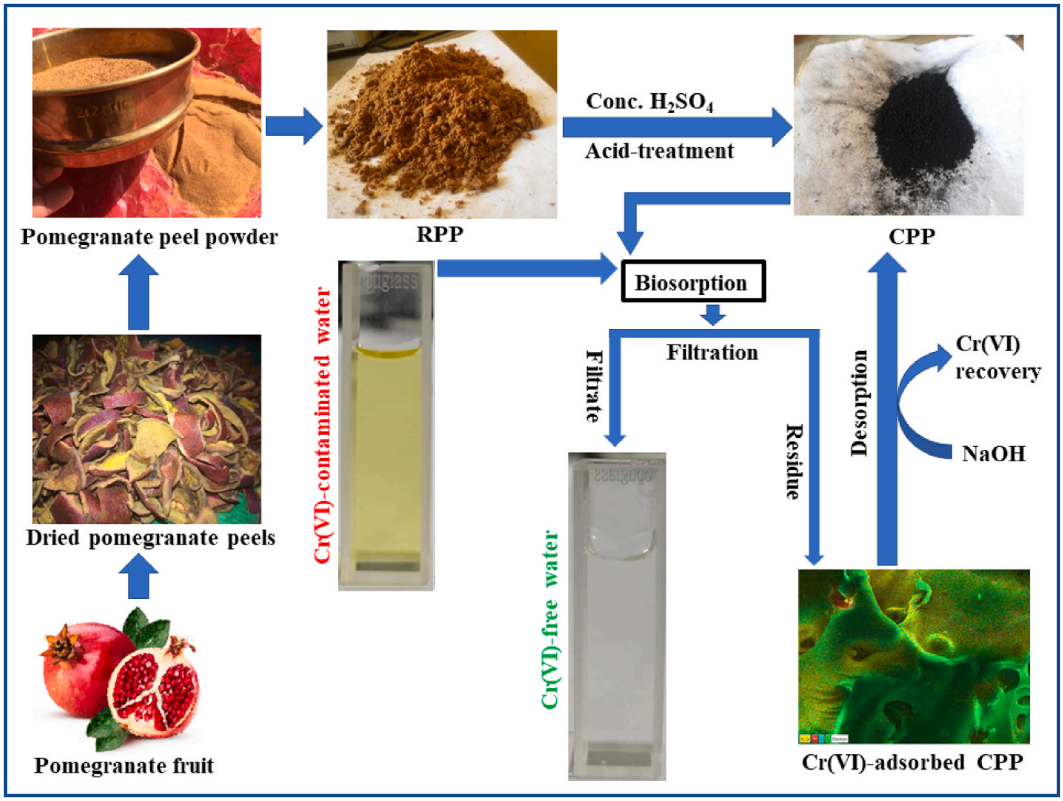

Scheme 2. Flowsheet showing the biosorbent synthetic route and Cr(VI) adsorption-desorption process.

Concentrated sulfuric acid was used to treat the dry RPP powder at a solid-liquid ratio of 1:2 g/mL. The biomass (RPP) is rich in cellulose content, and the acid modification of the adsorbent provides favorable conditions for the cellulose ring opening. Also, this causes sufficient micro-porosity and raises the surface area of the adsorbent [32]. The RPP's cellulose, hemicellulose, and lignin all have hydroxy surface functional groups that are meant to be activated by the modification. The charring mechanism is schematically shown in Scheme 1. The modified adsorbent was then washed until neutral pH and oven dried. The product thus obtained was named cross-linked pomegranate peel (CPP), which was further sieved to 220 μm and stored for its use during the experiment.

2.3. Adsorbent characterization

Identification of the point of zero charges (pH_{PZC}) value of the adsorbent (CPP) was carried out by using a Zeta potential analyzer (HORIBA Scientific SZ-100). The biosorbents' shape and elemental composition were examined using SEM pictures and EDS (JEOL JSM-6700F, Jeol Ltd., Tokyo, Japan). The surface functional groups of RPP, CPP, and Cr(VI)-adsorbed CPP were examined by using FTIR spectroscopy (IR AFFINITY-1 Shimadzu, Kyoto, Japan). XRD (Rigaku Ultima IV X-ray diffractometer (Rigacu Co., Japan) with Cu K_α ($\lambda = 1.54056$ A^o) radiation was employed to analyze the crystal structures of the adsorbents.

2.4. Biosorption experiments

Exactly 40 mL of known initial concentration with 40 mg of the adsorbent was taken in a volumetric flask for the adsorption studies of both RPP and CPP. At room temperature (298 ± 0.5K), the mixture was shaken for 24 h at 150 rpm to achieve equilibrium. After filtering the solution, the filtrates obtained were used to measure the residual chromium ion concentration. The initial, as well as residual Cr(VI) concentrations in aqueous samples (1–500 mg/L), were analyzed by an Inductively Coupled Plasma – Optical Emission Spectrometer (PerkinElmer Avio 220Max, ICP-OES). The calibration solutions were prepared by ICP standards of Cr (1000 mg/L, Sigma-Aldrich). To measure the concentration in the ppb level (0.2–1000 ppb), an Inductively Coupled Plasma – Mass Spectrometer (ICP-MS) (Agilent Technologies, 7900 ICP-MS, Santa Clara, CA, USA) was used. Batch biosorption tests conducted at different variables of solution pH, contact time, and initial metal ion concentrations at room temperature gave equilibrium data. Each trial was repeated thrice, and an average was calculated.

Equations (1) and (2) were employed to find out the biosorption capacity at equilibrium (q_e (mg/g)) and efficiency of biosorption in percentage.

$$q_e(\mathrm{mg/g}) = \frac{C_o - C_e}{M} \times V \tag{1}$$

$$\text{Biosorption efficiency } (\%) = \frac{C_o - C_e}{C_o} \times 100 \tag{2}$$

Where C_e denotes the equilibrium time concentrations of Cr(VI) in mg/L, C_o denotes the initial concentration in mg/L, M denotes the mass of the biosorbent in grams, and V represents the volume of the solution in liters [34,35]. The methodology for the preparation of the CPP and Cr(VI) adsorption-desorption process is schematically shown in Scheme 2.

2.4.1. Isotherm study

The Langmuir isotherm model explains the monolayer adsorption on the surface of the bio-adsorbent. It is expressed linearly as well as non-linearly by Equations (3) and (4), respectively [36].

$$q_e = \frac{q_{max}.b.C_e}{1 + b.C_e} \tag{3}$$

$$\frac{C_e}{q_e} = \frac{1}{q_{max}.b} + \frac{C_e}{q_{max}} \tag{4}$$

where, b denotes the Langmuir constant in L/mg, and q_{max} represents the maximum biosorption capacity in mg/g.

The Freundlich isotherm explains the multilayer adsorption on the heterogenous surface of the adsorbent. Equation (5) (non-linear) and Equation (6) (linear) are used to express this model [37].

$$q_e = KF\ (Ce)1/n \tag{5}$$

$$log\ q_e = log\ KF + log\ Ce \tag{6}$$

'K_F'; the Freundlich constant represents the biosorption capacity in (mg/g) $(\mathrm{L/mg})^{1/n}$, and 'n'; the Freundlich exponent represents the intensity of biosorption.

Furthermore, the study applied a separation factor (R_L) to describe the Langmuir model's important features which were defined by Equation (7).

$$R_L = \frac{1}{1 + b.C_o} \tag{7}$$

The Langmuir isotherm at constant temperature is implied by the R_L value. The R_L value of 1 suggests the linear Langmuir isotherm, the R_L value of 0 indicates irreversible sorption, whereas, values greater than 1 refer to unfavorable sorption, and values between 0 and 1 indicate favorable adsorption [38].

2.4.2. Adsorption kinetics

The kinetics of Cr(VI) adsorption on the biosorbent was determined by pseudo-first-, pseudo-second-order, and intra-particle diffusion models, which revealed the controlling mechanism. Equation (8) expresses the pseudo-first-order linear equation [39].

$$log(q_e - q_t) = log\ q_e - \times t \tag{8}$$

Where, k_1 in mg/g.min is the pseudo-first-order rate constant, while q_t in mg/g is the adsorption capacity at time t. Equation (9) represents the pseudo-second-order linear equation [40] as,

$$\frac{t}{q_t} = \frac{1}{k_2 {q_e}^2} + \frac{1}{q_e} \times t \tag{9}$$

where k_2 in g/mg. min is the pseudo-second-order rate constant [35].

The Weber-Morris intraparticle diffusion model [41] (Equation (10)) and Boyd's equations (Equations (11) and (12)) were used to assess the kinetics data to clarify the diffusion mechanism.

$$q_t = \left(K_{id} \times t^{0.5}\right) + C \tag{10}$$

$$\frac{q_t}{q_e} = 1 - \frac{6}{\pi^2}.\exp(-B_t) \tag{11}$$

$$B_t = -0.4977 - \ln\left(1 - \frac{q_t}{q_e}\right) \tag{12}$$

Where K_{id} denotes the rate constant of intraparticle diffusion in mg/g $\mathrm{min}^{-0.5}$, and C is the Weber-Morris equation intercept in mg/g. A Greater C value indicates a stronger boundary layer effect.

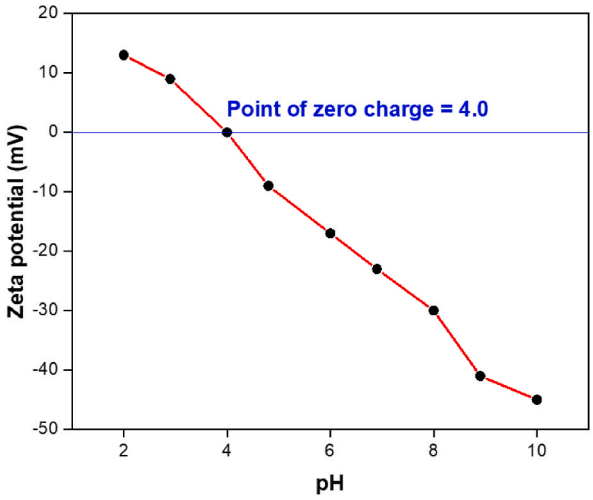

Fig. 1. Zeta potential of CPP.

2.5. Thermodynamic studies

Isotherm constants and experimental data at 298K, 308K, and 318K were employed to calculate the change in thermodynamic parameters (entropy (ΔS°), enthalpy (ΔH°), and Gibbs free energy (ΔG°)). The ΔG° values in KJ/mol of the adsorption process were determined using Equation (13).

$$\Delta G^\circ = -\mathrm{RT}\ \ln \mathrm{KC} \tag{13}$$

where K_C denotes the dimensionless thermodynamic equilibrium constant, R is the universal gas constant, and T is the temperature in kelvin. The value of K_C was determined by using the Langmuir constant (b) in L/mg. Considering the experiment to be performed in water, K_C can be expressed by Equation (14) [42–44].

$$\mathrm{KC} = \mathrm{b} \times 55.5 \times 1000 \times M_w \tag{14}$$

where $M_w = 52$ g/mol is the molar mass of chromium, and 55.5 is the number of moles of H_2O in 1 L of the solution.

Equation (15) shows the association of ΔG° with ΔS° and ΔH° at a given temperature.

$$\Delta G^\circ = \Delta H^\circ - T\Delta S^\circ \tag{15}$$

From Equation (13) and Equation (15), the following Van't Hoff equation (Equation (16)) is deduced:

$$\ln \mathrm{KC} = -\frac{\Delta H^\circ}{RT} + \frac{\Delta S^\circ}{R} \tag{16}$$

2.6. Desorption followed by reusability of CPP

Metal ion solution (100 mL) of a known concentration and optimum pH was treated with 100 mg of CPP and was agitated for 24 h. The adsorbed amount of the CPP was then computed by obtaining the equilibrium concentration. Exactly 50 mL of varying concentrations of NaOH solution were combined with the residue and agitated for about 24 h. The solution was then filtered, keeping the residue for further desorption. The percentage desorption (% D) of the metal ions is expressed by Equation (17).

$$\%\ \mathrm{D} = \times\ 100 \tag{17}$$

Where A_d denotes the desorbed amount and A_a is the amount of metal ions adsorbed in mg/g [45,46].

3. Results and discussion

3.1. Characteristics and chemical composition

Fig. 1 shows the zeta potential values of CPP at variable pH. It was observed that these values tend to decrease with the increase in pH. The point of zero charges (pH_{PZC}) of the CPP was determined to be 4.0. It indicates that the adsorption of anionic species of the hexavalent chromium is more favorable at a pH lower than 4.0 [47]. The electrostatic interaction of the anions with the adsorbent's positively charged surface promotes the adsorption of anionic species when the pH of the solution is less than pH_{PZC} whereas, when the

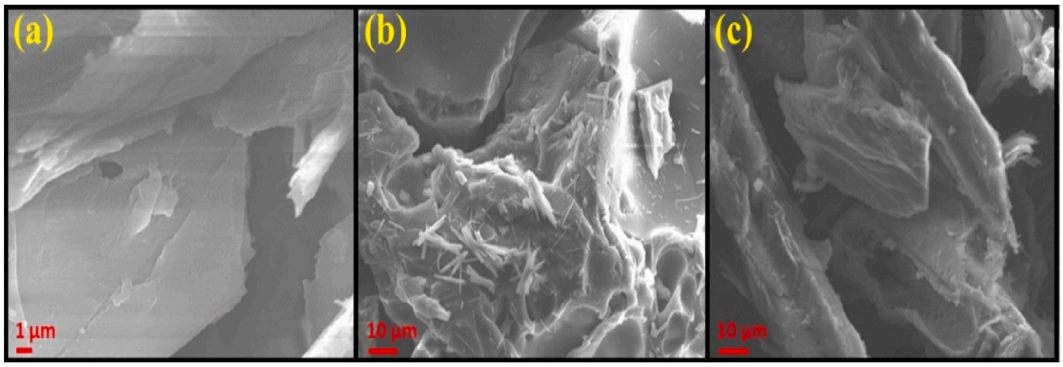

Fig. 2. SEM images of (a) RPP, (b) CPP, and (c) Cr(VI) adsorbed CPP.

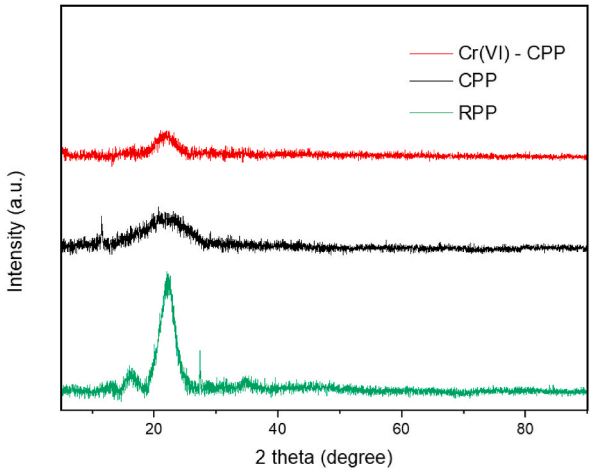

Fig. 3. XRD pattern of RPP, CPP, and Cr(VI) adsorbed CPP at 2 theta.

pH is larger than pH_{PZC}, the adsorption of cationic species is preferred.

Fig. 2 shows the SEM images of RPP, CPP, and Cr(VI) loaded CPP. The smooth, homogenous surface of the RPP (Fig. 2(a)) was discovered to contain significantly fewer pores and voids. Whereas the CPP (Fig. 2(b)) showed rough surfaces with more cavities and pores due to the acid modification process. The metal-loaded CPP (Fig. 2(c)) showed decreased surface roughness due to the adsorption of Cr(VI) ions.

The amorphous biosorbent surface is comparatively more suitable for metal loading than a crystalline surface. XRD diffractogram (Fig. 3) showed an intense peak at 2 θ around 22 ° to 24 ° in RPP, illustrating the presence of crystalline cellulose. On the other hand, the peak intensity is noticeably reduced in the case of CPP. This signified that CPP possessed improved amorphous structure due to acid treatment. Furthermore, a broader peak of CPP indicated a smaller particle size, facilitating the adsorption sites to better capture the adsorbate species. This showed that CPP was more likely for metal sorption. The peak was further narrowed in Cr(VI)-adsorbed CPP, which might be due to the increase in particle size after the Cr(VI) uptake.

The EDS analysis was used to determine the Cr(VI)-adsorbed CPP's elemental composition. EDS electron image in Fig. 4(a) and layered image in Fig. 4(b) showed that the elements are heterogeneously distributed on the surface of the biosorbent. Carbon, oxygen, silicon, and chromium were all visible by color mapping of the overlapping components in Fig. 4(c) and (d) revealed that the Cr(VI)-adsorbed CPP included a higher content of carbon and oxygen along with 3.99% abundance of chromium.

Fig. 5 displays the FTIR spectra of RPP, CPP, and Cr(VI) adsorbed CPP ranging from 4000 cm^{-1} to 500 cm^{-1}. The broad peak at 3333 cm^{-1} in RPP indicates the presence of hydroxyl (-OH) groups of cellulose, hemicellulose, and lignin. This peak disappeared after the acid modification. A peak at 2924 cm^{-1} in CPP and RPP can be due to –CH stretching vibrations. This peak disappeared after the Cr (VI) intake. The carbonyl stretching vibration caused the appearance of peaks at 1620.21 cm^{-1} and 1728.22 cm^{-1} in RPP, which shifted to 1697.36 cm^{-1} in CPP and the peak disappeared in Cr(VI)-adsorbed CPP, indicating the Cr(VI) adsorption on the adsorbent surface. The effective chemical modification of RPP into CPP and the potent Cr(VI) adsorption on the CPP were suggested by all the aforementioned factors.

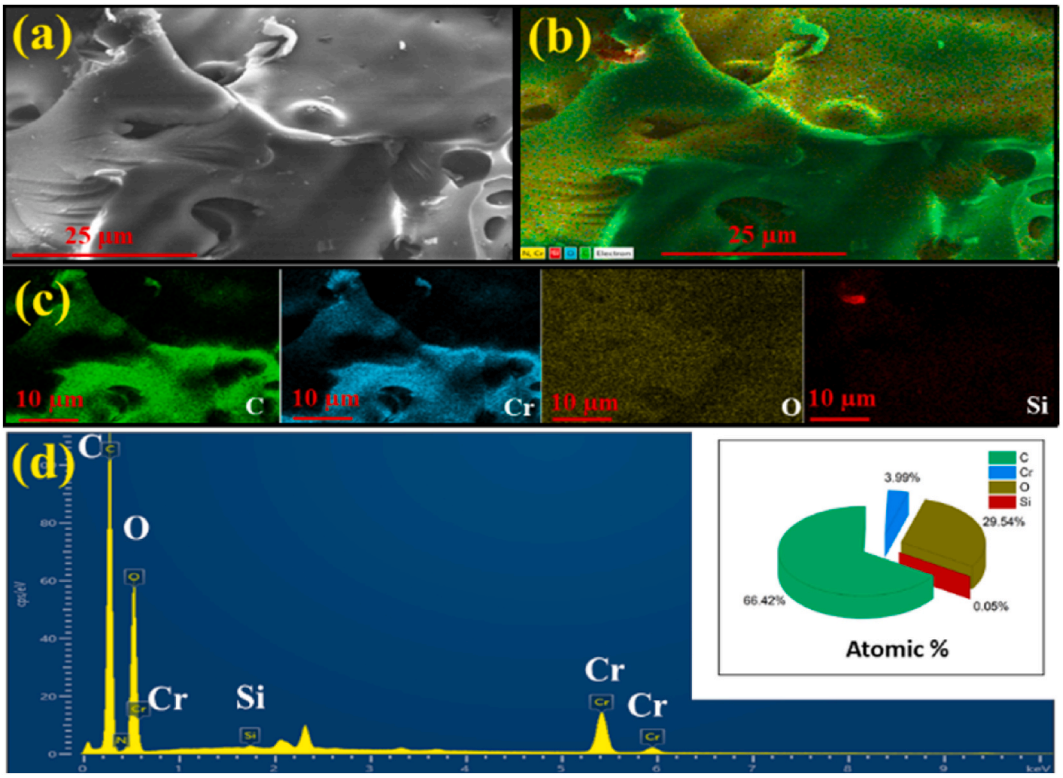

Fig. 4. (a) Electron picture from EDS, (b) layered picture, (c) color mapping of overlapping elements, and, (d) the elemental distribution of Cr(VI)-adsorbed CPP shown by its atomic percentage.

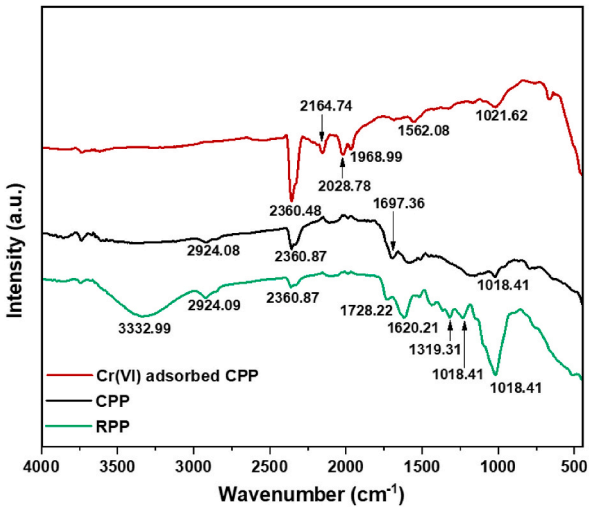

Fig. 5. FTIR spectrum of the RPP, CPP, and Cr(VI) adsorbed CPP.

3.2. Impact of solution pH

The adsorption of Cr(VI) onto the RPP and CPP was studied in the pH range of 1–7. At natural pH conditions (pH = 7), CPP showed a Cr(VI) removal efficiency of 29.41% whereas, RPP had only 10.25%. Removal efficiencies of both RPP and CPP increased from pH 1 to 2 and then decreased with the further rise in pH. The ideal pH for maximum Cr(VI) removal by both CPP and RPP was determined to be 2.0. Fig. 6 shows the maximal removal of chromium at a pH of 2.0 being 25.46% for RPP and 96.10% for CPP. Due to a huge difference between the removal efficiencies of RPP and CPP, further studies were carried out for the CPP only. Similar results for the

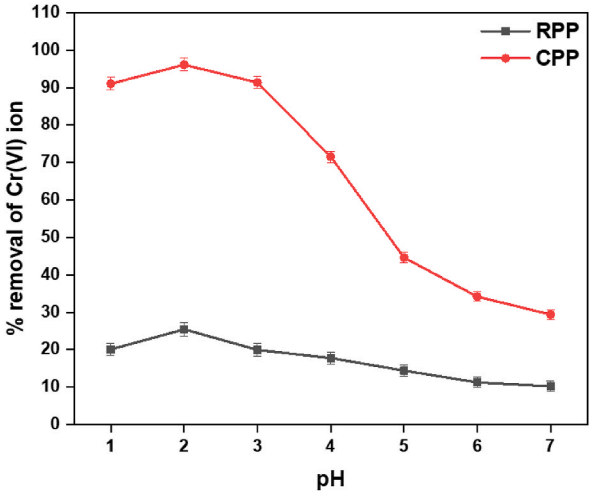

Fig. 6. Impact of solution pH on Cr(VI) adsorption by RPP and CPP.

Table 1
Cr(VI) composition with pH.

pH	Most common types of Cr (VI)
Below 1	H_2CrO_4
2 tso 4	$Cr_2O_7^{2-}$
4 to 6	$HCrO_4^-$, $Cr_2O_7^{2-}$
6 to 8	$Cr_2O_7^{2-}$, CrO_4^{2-}
Above 8	CrO_4^{2-}

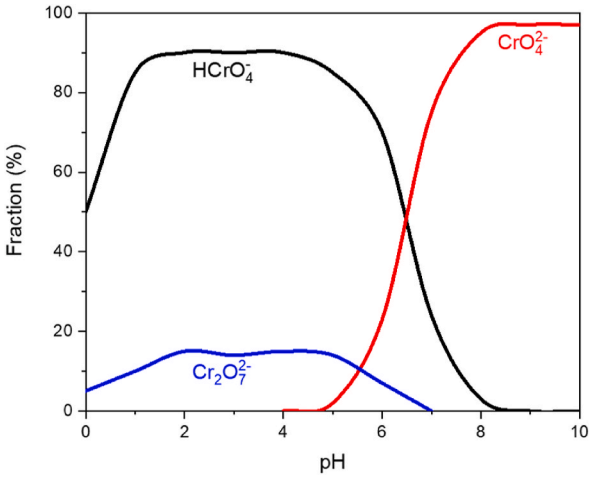

Fig. 7. Speciation graph of Cr(VI) at variable pH values.

hexavalent chromium removal using bio-adsorbents have been reported in previous studies with the optimum pH being 2.0 [9,11, 48–50].

Cr(VI) chemistry is highly reliant on pH. Table 1 lists the predominant Cr(VI) species for each pH range [51].

In a basic medium, it forms CrO_4^{2-} ions whereas, in an acidic medium (pH 1 to 6), $HCrO_4^-$ and $Cr_2O_7^{2-}$ ions are in equilibrium, $HCrO_4^-$ being the most common species. At pH below 1, H_2CrO_4 is the dominating species [24,42,52]. A very high positive redox potential for Cr (VI) in an acidic solution implies that it is strongly oxidizing in the presence of species that donate electrons. $HCrO_4^-$ is the prevalent form of hexavalent chromium at a pH value of 2–6. The surface protonation of the adsorbent results in the creation of a positive charge on the adsorbent surface because the solution contains a large number of H^+ ions in this pH range. $HCrO_4^-$ is significantly adsorbed onto these positively charged surfaces as a result of their electrostatic interaction with the Cr(VI) anion. Consequently, in this pH range, adsorption is more favorable [53]. However, at greater pH values, the percentage adsorption of Cr(VI) sharply declines as a higher

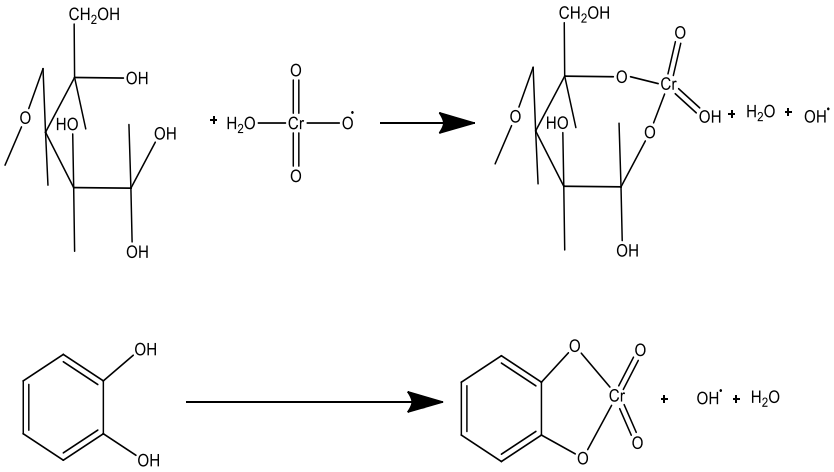

Scheme 3. Complexation of Cr(VI) with cellulose and polyphenolic/polyhydroxy functional moiety contained in pomegranate peel [55].

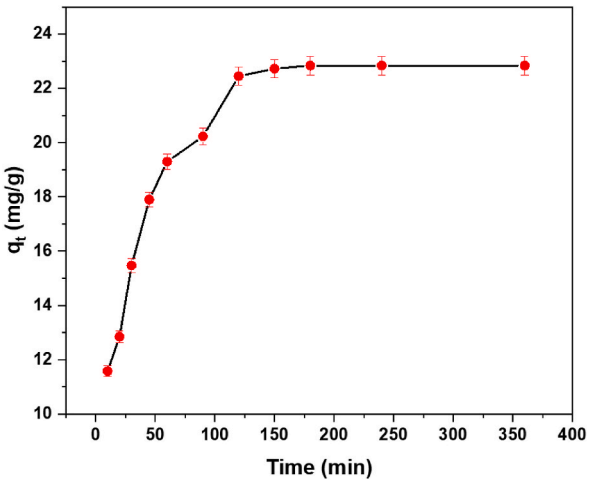

Fig. 8. Impact of contact time on biosorption of Cr(VI) onto CPP.

concentration of hydroxyl ions strongly contends with CrO_4^{2-} ions for the adsorption site [52]. At pH less than 2, there is an extremely high concentration of H^+ ions, encouraging the reduction of Cr(VI) to Cr(III). Hence, there is a decline in the adsorption of Cr(VI) at pH values lower than 2 [42]. Moreover, the coexistence of $Cr_2O_7^{2-}$ and CrO_4^{2-} with $HCrO_4^-$ in the solution medium, which results in their competition on the adsorption sites, is the cause of the decrease in the rate of adsorption [24,47]. Fig. 7 illustrates the speciation graph of Cr(VI) at various pH values [54].

Figure: 7. From the pH studies, the RPP was observed to be comparatively less significant in comparison to the CPP for the adsorption of Cr(VI), due to which further studies were carried out using only the CPP. The complexation mechanism of Cr(VI) with cellulose and polyphenolic/polyhydroxy functional moiety contained in pomegranate peel is schematically shown in Scheme 3.

3.3. Impact of contact time on adsorption of Cr(VI) onto CPP

The batch biosorption of a 50 ppm Cr(VI) solution with 25 mg of the adsorbent was studied by assessing the influence of contact time throughout time intervals ranging from 10 min to 24 h. Fig. 8 shows the adsorption of Cr(VI) onto CPP and RPP from 10 min to 24 h. Adsorption of chromium and adsorption percentages of chromium onto CPP was found to be constant after 180 min, indicating the equilibrium time for the maximum adsorption.

3.4. Adsorption kinetics studies

To assess the kinetic data for the adsorption of chromium ions onto CPP, pseudo-first-order and pseudo-second-order kinetic models were used. After analyzing these plots in Fig. 9, it was determined that the pseudo-second-order model, which had a higher correlation

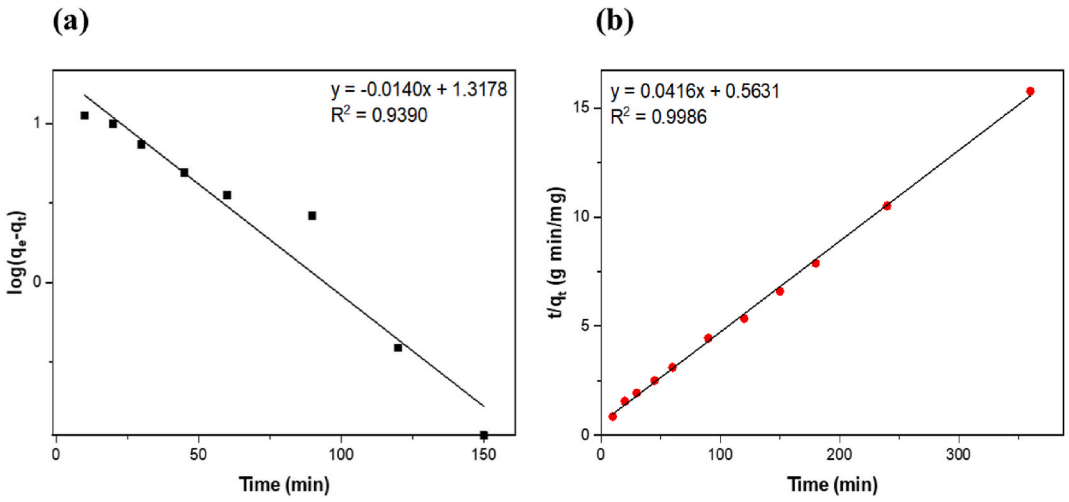

Fig. 9. (a) Pseudo-first-order and, (b) Pseudo-second-order kinetic models for the adsorption of Cr(VI) onto CPP.

Table 2
Kinetic parameter determined for the biosorption of Cr(VI) onto CPP at pH 2.0.

q_{exp}(mg/g)	Pseudo-first order			Pseudo-second order		
	K_1 (min^{-1})	q_e(mg/gm)	R^2	K_2(mg/g/min)	q_e(mg/gm)	R^2
22.84	0.032	20.780	0.975	0.003	24.030	0.999

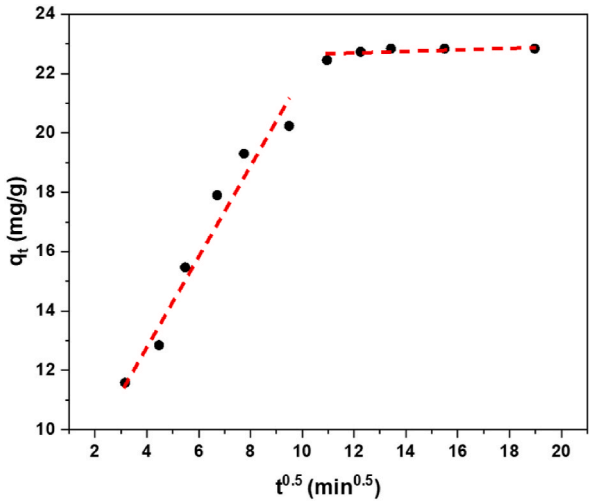

Fig. 10. Intraparticle diffusion model for the Cr(VI) biosorption on CPP.

coefficient (R^2) value than the pseudo-first-order kinetic model, best explained the adsorption of Cr(VI) onto CPP, suggesting that the Cr(VI) adsorption onto CPP may be driven by chemisorption. The results of the kinetic study were found to align with similar studies conducted previously, that used several biomass-based adsorbents for the adsorption of Cr(VI) ions [22,23]. The calculated kinetic parameter values are shown in Table 2.

Intra-particle diffusion has an important role in biosorption on a porous adsorbent [56]. To study the diffusion mechanism and rate-limiting step, a plot of q_t vs. $t^{0.5}$ (Fig. 10) was drawn. Adsorption is dominated by the intra-particle diffusion only when the plot is linear. The intra-particle diffusion is responsible for the rate-limiting process if the plot intersects the origin. The multi-linear plot in the study revealed that the adsorption mechanism was affected by two or more steps, and in addition to intra-particle diffusion, there were other mechanisms too, which determined the rate-limiting step [4,57]. Two different lines in the fitted model indicated two stages involved in the adsorption process. The first stage is external diffusion, which involved the transport of metal ions from the solution to the external surface of the CPP. The second is intra-particle diffusion, in which the chromium ions got diffused from the

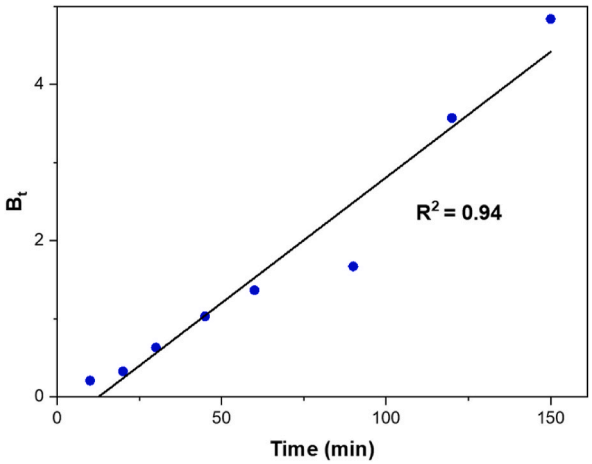

Fig. 11. Boyd's plot for Cr(VI) adsorption onto CPP.

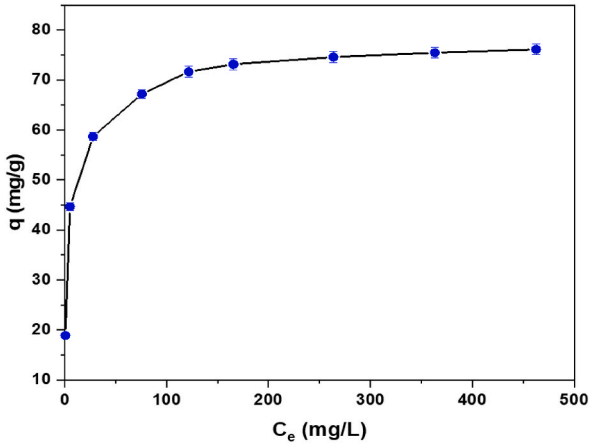

Fig. 12. Adsorption isotherm of Cr(VI) onto CPP.

surface into the pores of the CPP [23].

The results obtained from the Weber-Morris model were further verified by Boyd's model. If the B_t vs. t plot (Fig. 11) is linear and passes through the origin, the intra-particle diffusion governs the adsorption process. Otherwise, external diffusion (film diffusion) will be the rate-determining step [58]. Boyd's plot showed linearity but did not intersect the origin. This signified that film diffusion solely controlled the Cr(VI) adsorption rate onto CPP. Norouzi et al. employed Boyd's diffusion model and reported the film diffusion as the rate-limiting step for Cr(VI) adsorption onto agro waste-based activated carbon [59].

3.5. *Adsorption isotherm model*

The efficiency of CPP at a pH value of 2.0 was studied at varying concentrations (10.03 mg/L, 25.54 mg/L, 50.21 mg/L, 100.11 mg/L, 150.44 mg/L, 202.21 mg/L, 300.23 mg/L, 400.66 mg/L, and 500.52 mg/L) of Cr(VI) ions maintaining other parameters constant. From Fig. 12 it is evident that with the increase of the equilibrium concentration of Cr(VI) from 0.57 to 462.46 mg/L, the adsorption capacity increased from 18.92 to 82.99 mg/g.

To evaluate the best-fit isotherm model for biosorption, the experimental data of Cr(VI) adsorption onto CPP was analyzed using Langmuir and Freundlich isotherm equations. Linear plots were obtained in both models as shown in Fig. 13.a. and 13.b., respectively. The determined values of Freundlich and Langmuir parameters with their respective R^2 values have been listed in Table 3. The obtained correlation coefficient (R^2) value for Langmuir isotherm ($R^2 > 0.99$) was greater than that of Freundlich isotherm ($R^2 > 0.86$) for a pH value of 2.0. Hence, the adsorption model is best fitted by the Langmuir isotherm model. This indicates that the distribution of active sites on the adsorbent surface is homogeneous, and the adsorption is monolayer [36,60].

The maximal Cr(VI) adsorption capacity utilizing CPP examined in the present study has been compared with several other biosorbents described in various literature and is shown in Table 4. The results unmistakably demonstrate that CPP has the best Cr(VI) adsorption capacity among the described adsorbents, which suggests that CPP can be used as an effective biosorbent for the

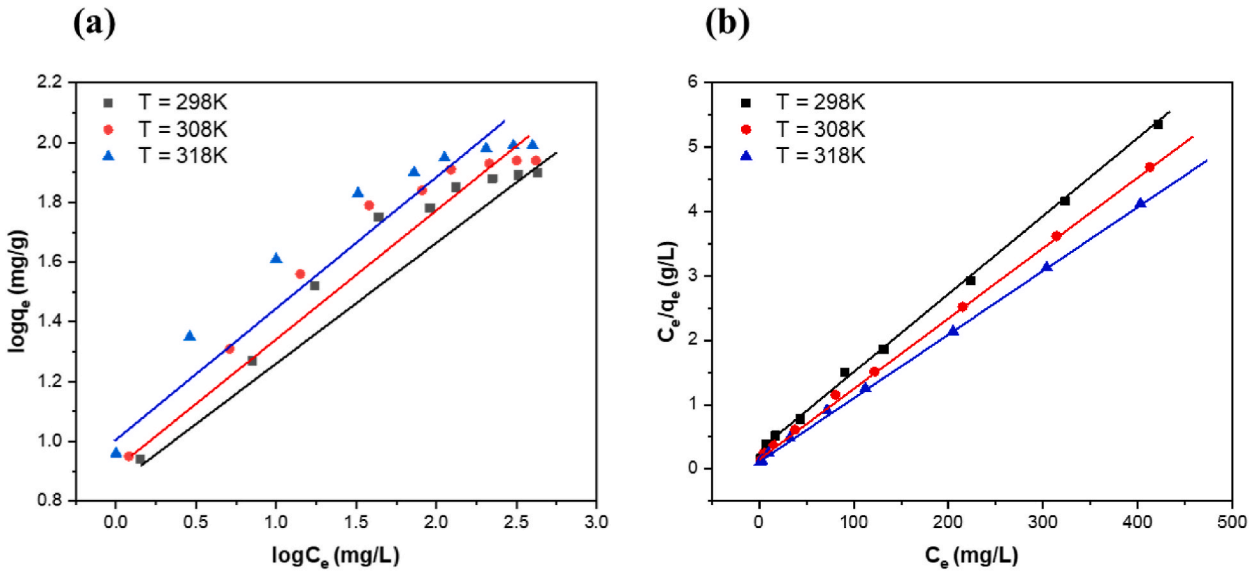

Fig. 13. (a) Linearized Langmuir isotherm plot, and (b) Linearized Freundlich isotherm plot of Cr(VI) adsorbed CPP at various temperatures.

Table 3
Langmuir and Freundlich parameters for Cr(VI) adsorption on CPP.

Isotherm Model	Parameter	298 K	308 K	318 K
Langmuir	q_m (mg g^{-1})	82.99	91.74	101.21
	b (L mg^{-1})	0.044	0.055	0.071
	R^2	0.998	0.999	0.999
Freundlich	K_F (mg g^{-1}) (L $mg^{-1})^{1/n}$	9.27	10.91	13.64
	N	2.54	2.57	2.67
	R^2	0.936	0.924	0.905

Table 4
Comparison of Cr(VI) biosorption capacities of several adsorbents with CPP.

SN	Bio-adsorbent	pH	Biosorption Capacity (mg/gm)	Reference
1	Pomegranate peel	3.0	28.28	(Abdel-Galil et al., 2021)
2	Walnut shell (diethyl triamine treated)	3.0	50.10	(Li et al., 2020)
3	Pomelo peel ($FeCl_3$ treated)	2.0	21.55	(Q. Wang et al., 2020)
4	*Citrus limetta* fruit waste (Fe modified)	3.0	2.00	(Pintor et al., 2018)
5	Sawdust (formaldehyde-treated)	2.0	8.84	(Chakraborty et al., 2021)
6	Betelnut powder	4.0	12.01	(Rahman et al., 2012)
7	Coconut husk	2.0	29.00	(Tan et al., 1993)
8	Fe^{3+}/Fe^{2+} black cumin seeds	5.0	15.75	(Thabede et al., 2021)
9	Rice husk (NaOH treated)	2.0	34.85	(Pant et al., 2022)
10	*Arundo donax* stem powder (H_2SO_4 treated)	2.0	76.92	(Bhattarai et al., 2022)
11	Pomegranate peel (H_2SO_4 treated)	2.0	82.99	Present study

sequestration of Cr(VI) ions from contaminated water.

3.6. Thermodynamic studies

The study evaluated the thermodynamic parameters from the adsorption isotherm studies of Cr(VI) onto CPP at different temperatures. Fig. 14 displays the Van't Hoff plot of lnK_C against 1/T, which was employed to determine the values of ΔH^0 and ΔS^0, and Table 5 demonstrates the evaluated thermodynamic parameter values. The negative values of ΔG^0 suggested that the biosorption process was feasible, spontaneous, and thermodynamically favorable [61]. The endothermic sorption process was suggested by the positive values of ΔH^0. Also, the q_m value was found to rise with the elevation in temperature. The positive values of ΔS^0 indicate the increase in randomness of Cr(VI) ions on the surface of CPP.

Fig. 15 demonstrates the variation of R_L values with initial concentrations at varying temperatures. From the experimental data, the values of R_L were determined between 0 and 1, indicating that the biosorption of Cr(VI) onto CPP is favorable and the bonding between

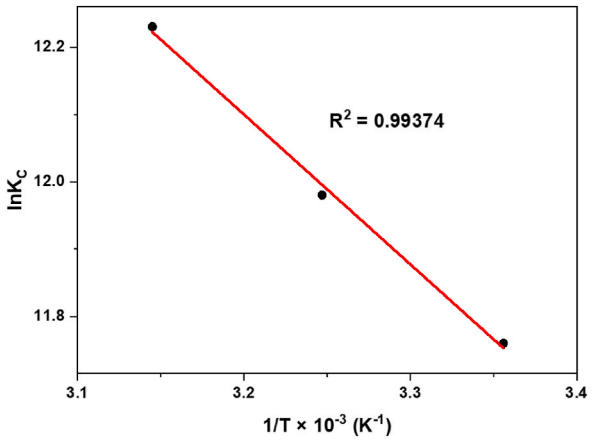

Fig. 14. Van't Hoff plot of 1/T Vs. $\ln K_C$.

Table 5
Thermodynamic parameters of CPP and Cr(VI) system.

T (K)	b (L/mol)	ΔG^0 (KJ/mol)	ΔH^0 (KJ/mol)	ΔS^0 (J/mol/K)
298	0.6507	−29.14		
308	0.9422	−30.68	33.43	232.16
318	1.5312	−32.34		

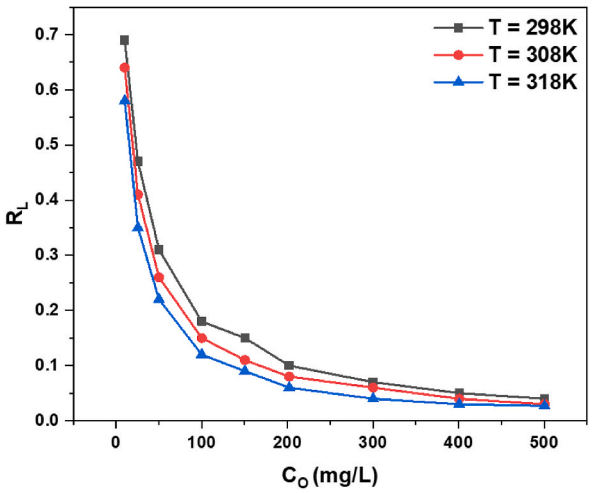

Fig. 15. R_L value as function of initial concentration of Cr(VI) at different temperatures.

Cr(VI) and the CPP surface is strong at all three temperatures of 298K, 308K, and 318K.

3.7. Impact of adsorbent dosage for the Cr(VI) adsorption

Fig. 16 shows the relationship between the dose of CPP and residual Cr(VI) concentrations. As per the limit set by WHO, the Cr(VI) concentration in drinking water should not exceed 0.05 mg/L. The outcome revealed that utilizing 1.2 g/L of CPP as an adsorbent caused the concentration of chromium to drop from 24 mg/L to 0.05 mg/L. The further increase in the concentration led to the complete removal of Cr(VI) from the aqueous solution. Due to the availability of surface-active sites, the amount of the metal ion that is adsorbed increases as the adsorbent dosage increases. The results are found agreeing to the findings of Pant et al. [23].

3.8. Desorption study and reusability of CPP

The direct disposal of Cr(VI) loaded adsorbent in the environment is hazardous. For this, a method of regeneration of the bio-

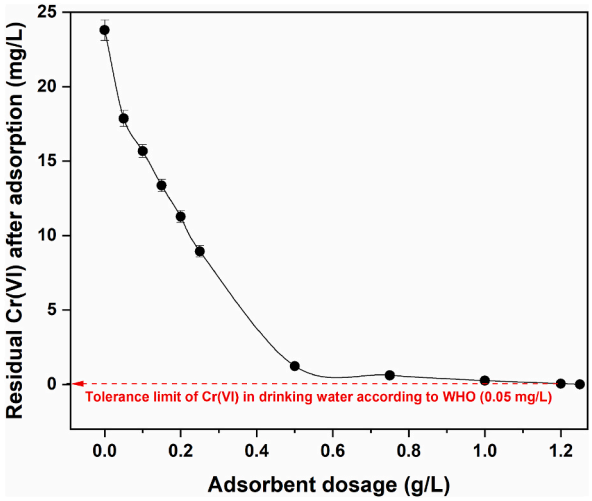

Fig. 16. Impact of the adsorbent dosage on biosorption of Cr(VI) onto CPP at pH 2.0.

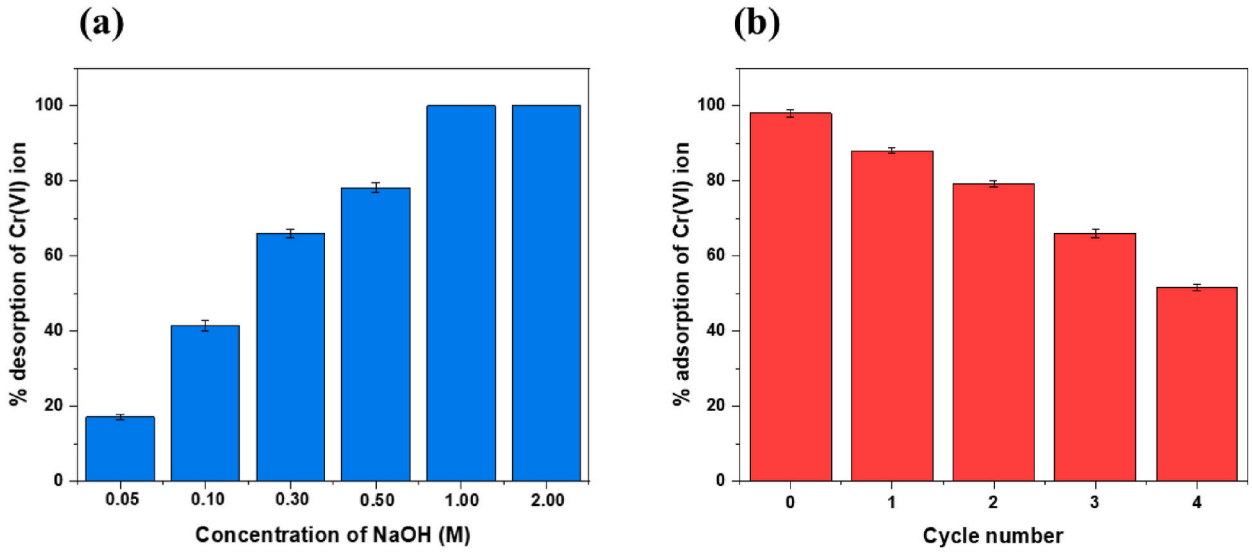

Fig. 17. (a) Cr(VI) desorption percentage Vs. molar concentration of NaOH and (b) Variation of the biosorption ability of CPP in several adsorption-desorption cycles.

adsorbent (CPP) simultaneously disposing of the contaminated solution has been studied. Based on various literature studies, NaOH has been considered best for the desorption of Cr(VI) from bio-adsorbents [31,62]. From the study of the impact of solution pH (Fig. 6), it is clear that Cr(VI) can be easily loaded onto CPP at lower pH whereas, an increase in pH undermines the Cr(VI) uptake ability of the adsorbent. This allowed the use of an alkaline solution as an eluent for the desorption process. The present investigation used varying concentrations of NaOH solution as an eluent for the desorption study. The effect of eluent concentration on CPP is shown in Fig. 17(a). The experiment demonstrated that as the concentration of NaOH was increased from 0.05 to 1.00 M, the desorption percentage climbed from 17.13% to 98.04% and stayed consistent as the concentration increased further. It signifies the optimum concentration of the NaOH for the desorption is 1.0 M. Fig. 17(b) shows the performance of CPP after some adsorption-desorption cycles. The efficiency of removal was 88.12% in the first cycle, which decreased to 79.34%, 66%, and 51.67% in the second to fourth cycles, respectively. The results showed that CPP can be effectively regenerated for its reuse for some cycles. The decrease in the removal efficiency may be due to: (a) blockage of some pores of the adsorbent; (b) decreased number of active sites on the biosorbent surface due to the complex formed between Cr(VI) and the functional groups [63]. The desorption mechanism of Cr(VI) is shown in Scheme 4.

Cr(VI) thus being desorbed is harmful to the environment, so it should be safely disposed of. The bio-adsorbed Cr(VI) was precipitated as the hydroxide of chromium ($Cr(OH)_3$), which was further calcined at the elevated temperature of 1200 $^{\circ}C$ to obtain chromium oxide (Cr_2O_3). This oxide of chromium can easily be dissolved in acids such as H_2SO_4 and can be used in the tannery. Also, it can be used for the manufacture of other chromium compounds [64]. Reactions involved in Cr(VI) recovery steps are as follows,

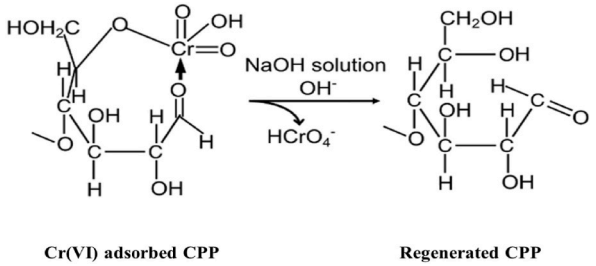

Scheme 4. Desorption mechanism of Cr(VI) from Cr(VI) - adsorbed CPP [66].

$$Cr^{3+} + 3\mathrm{OH}^- \rightarrow Cr(OH)_3$$

$$2\ Cr(OH)_3 \xrightarrow{(T=1200^\circ C)} Cr_2O_3 + 3H_2O$$

$$Cr_2O_3 + 3H_2SO_4 \rightarrow Cr(SO_4)_3 + 3H_2O$$

Another alternative to disposing of the metal-loaded adsorbent is by heating it [65]. The Cr(VI) adsorbed CPP was heated at about 650 $^\circ C$, generating ashes, followed by the leaching test. After a day, no percolation of Cr(VI) indicated the ash was safe. The outcome suggested that the metal loaded CPP can be securely utilized as fuel.

4. Conclusions

The current work demonstrates that acid-treated pomegranate peels can be employed to remove hexavalent chromium from water in an efficient manner. Tools like EDS, SEM, XRD, and FTIR were employed for the characterization of the adsorbent. The biomass was amorphous with rough and porous surfaces, which later got occupied after Cr(VI) adsorption. The pH_{PZC} of the adsorbent was determined to be 4.0. Several parameters including contact time, adsorbent dose, and solution pH were examined in a batch method to determine the effectiveness of the sorbent. The maximum adsorption (q_m) was found to be 82.99 mg/g at 298K with an optimum contact time of 180 min. The isotherm data were following the Langmuir adsorption model and the kinetic data supported the pseudo-second-order model. The biosorbent was found to be regenerable for several cycles by desorption study of Cr(VI) from the Cr(VI) loaded CPP using NaOH as a regenerant. The recovered metal had a good potential for its use in the tannery and the manufacture of other chromium compounds. Also, the spent adsorbent was easily and safely disposed of by burning it as fuel. This study demonstrates that chemically modified pomegranate peel powder is more significant in the uptake of Cr(VI) in comparison to the raw adsorbent. On the other hand, the negative impact of sulfuric acid on the environment necessitates the study and development of comparatively benign bio-adsorbents. The present research was carried out on a laboratory scale using batch adsorption methods. There is a necessity for further research in continuous column mode in a real environment for the development of large-scale applications of the adsorbent.

Acknowledgment

The authors are grateful to Mr. Dasu Ram Poudel, and Mr. Prakash Chandra Lohani (Jeonbuk National University, Jeonju, South Korea) for FE-SEM and EDX analysis.

References

[1] E.I. Unuabonah, C. Günter, J. Weber, S. Lubahn, A. Taubert, Hybrid clay: a new highly efficient adsorbent for water treatment, ACS Sustain. Chem. Eng. 1 (2013) 966–973, https://doi.org/10.1021/sc400051y.
[2] M. Agarwal, K. Singh, Heavy metal removal from wastewater using various adsorbents: a review, J. Water Reuse Desalin. 7 (2017) 387–419, https://doi.org/10.2166/wrd.2016.104.
[3] S. Saraswat, J.P.N. Rai, Heavy metal adsorption from aqueous solution using *Eichhornia crassipes* dead biomass, Int. J. Miner. Process. 94 (2010) 203–206, https://doi.org/10.1016/j.minpro.2010.02.006.
[4] A.E.D. Mahmoud, Graphene-based nanomaterials for the removal of organic pollutants: Insights into linear versus nonlinear mathematical models, J. Environ. Manag. 270 (2020), 110911, https://doi.org/10.1016/j.jenvman.2020.110911.
[5] E. Suganya, N. Saranya, C. Patra, L.A. Varghese, N. Selvaraju, Biosorption potential of *Gliricidia sepium* leaf powder to sequester hexavalent chromium from synthetic aqueous solution, J. Environ. Chem. Eng. 7 (2019), 103112, https://doi.org/10.1016/j.jece.2019.103112.
[6] I. Moffat, N. Martinova, C. Seidel, C.M. Thompson, Hexavalent chromium in drinking water, J. Am. Water Works Assoc. 110 (2018) E22–E35, https://doi.org/10.1002/awwa.1044.
[7] Y. Chen, D. An, S. Sun, J. Gao, L. Qian, Reduction and removal of chromium VI in water by powdered activated carbon, Materials 11 (2018) 1–12, https://doi.org/10.3390/ma11020269.
[8] Ş. Parlayici, E. Pehlivan, Comparative study of Cr(VI) removal by bio-waste adsorbents: equilibrium, kinetics, and thermodynamic, J. Anal. Sci. Technol. 10 (2019), https://doi.org/10.1186/s40543-019-0175-3.
[9] M. Bansal, D. Singh, V.K. Garg, A comparative study for the removal of hexavalent chromium from aqueous solution by agriculture wastes' carbons, J. Hazard Mater. 171 (2009) 83–92, https://doi.org/10.1016/j.jhazmat.2009.05.124.
[10] F. Gode, E. Pehlivan, Removal of Cr(VI) from aqueous solution by two Lewatit-anion exchange resins, J. Hazard Mater. 119 (2005) 175–182, https://doi.org/10.1016/j.jhazmat.2004.12.004.

[11] T. Karthikeyan, S. Rajgopal, L.R. Miranda, Chromium(VI) adsorption from aqueous solution by *Hevea Brasilinesis* sawdust activated carbon, J. Hazard Mater. 124 (2005) 192–199, https://doi.org/10.1016/j.jhazmat.2005.05.003.

[12] R.R. Patterson, S. Fendorf, M. Fendorf, Reduction of hexavalent chromium by amorphous iron sulfide, Environ. Sci. Technol. 31 (1997) 2039–2044, https://doi.org/10.1021/es960836v.

[13] E. Rathore, K. Maji, K. Biswas, Nature-Inspired Coral-like Layered $[Co_{0.79}AI_{0.21}(OH)_2(Co_3)_{0.11}].mH_2O$ for fast selective ppb level capture of Cr(VI) from contaminated water, Inorg. Chem. 60 (2021) 10056–10063, https://doi.org/10.1021/acs.inorgchem.1c01479.

[14] W. Mertz, Chromium in human nutrition: a review, J. Nutr. 123 (1993) 626–633, https://doi.org/10.1093/jn/123.4.626.

[15] D. Mohan, C.U. Pittman, Activated carbons and low cost adsorbents for remediation of tri- and hexavalent chromium from water, J. Hazard Mater. 137 (2006) 762–811, https://doi.org/10.1016/j.jhazmat.2006.06.060.

[16] M.R. Pokhrel, B.R. Poudel, R.L. Aryal, H. Paudyal, K.N. Ghimire, Removal and recovery of phosphate from water and wastewater using metal-loaded agricultural waste-based adsorbents: a review, J. Instr. Sci. Technol. 24 (2019) 77–89, https://doi.org/10.3126/jist.v24i1.24640.

[17] M.R. Adam, N.M. Salleh, M.H.D. Othman, T. Matsuura, M.H. Ali, M.H. Puteh, A.F. Ismail, M.A. Rahman, J. Jaafar, The adsorptive removal of chromium (VI) in aqueous solution by novel natural zeolite based hollow fibre ceramic membrane, J. Environ. Manag. 224 (2018) 252–262, https://doi.org/10.1016/j.jenvman.2018.07.043.

[18] R.M. Sedman, J. Beaumont, T.A. McDonald, S. Reynolds, G. Krowech, R. Howd, Review of the evidence regarding the carcinogenicity of hexavalent chromium in drinking water, J. Environ. Sci. Health Part C Environ. Carcinog. Ecotoxicol. Rev. 24 (2006) 155–182, https://doi.org/10.1080/10590500600614337.

[19] Y. Zhang, G. Lan, Y. Liu, T. Zhang, H. Qiu, F. Li, J. Yan, Y. Lu, Enhanced adsorption of Cr (VI) from aqueous solution by zirconium impregnated chitosan microspheres: mechanism and equilibrium, Separ. Sci. Technol. 56 (2021) 2532–2545, https://doi.org/10.1080/01496395.2020.1842451.

[20] B. Wang, Z. Li, Q. Lang, M. Tan, C. Ratanatamskul, M. Lee, Y. Liu, Y. Zhang, A comprehensive investigation on the components in ionic liquid-based polymer inclusion membrane for Cr(VI) transport during electrodialysis, J. Membr. Sci. 604 (2020), 118016, https://doi.org/10.1016/j.memsci.2020.118016.

[21] H. Karimi-Maleh, A. Ayati, S. Ghanbari, Y. Orooji, B. Tanhaei, F. Karimi, M. Alizadeh, J. Rouhi, L. Fu, M. Sillanpää, Recent Advances in Removal Techniques of Cr(VI) Toxic Ion from Aqueous Solution: A Comprehensive Review, 2021, https://doi.org/10.1016/j.molliq.2020.115062.

[22] K.P. Bhattarai, B.D. Pant, R. Rai, R.L. Aryal, H. Paudyal, S.K. Gautam, K.N. Ghimire, M.R. Pokhrel, B.R. Poudel, Efficient sequestration of Cr(VI) from aqueous solution using biosorbent derived from *Arundo donax* stem, J. Chem. 2022 (2022), https://doi.org/10.1155/2022/9926391.

[23] B.D. Pant, D. Neupane, D.R. Paudel, P. Chandra Lohani, S.K. Gautam, M.R. Pokhrel, B.R. Poudel, Efficient biosorption of hexavalent chromium from water by modified arecanut leaf sheath, Heliyon 8 (2022), https://doi.org/10.1016/j.heliyon.2022.e09283.

[24] R. Rai, D.R. Karki, K.P. Bhattarai, B. Pahari, N. Shrestha, S. Adhikari, S.K. Gautam, B.R. Poudel, Recent advances in biomass-based waste materials for the removal of chromium (VI) from wastewater: a review, Amrit Res. J. 2 (2021) 37–50, https://doi.org/10.3126/arj.v2i01.40736.

[25] R.L. Aryal, B.R. Poudel, S.K. Gautam, H. Paudyal, K.N. Ghimire, Removal of fluoride from aqueous solution using biomass-based adsorbents: a review, J. Nepal Chem. Soc. 40 (2019) 44–51, https://doi.org/10.3126/jncs.v40i0.27281.

[26] B.R. Poudel, R.L. Aryal, S. Bhattarai, A.R. Koirala, S.K. Gautam, K.N. Ghimire, B. Pant, M. Park, H. Paudyal, M.R. Pokhrel, Agro-waste derived biomass impregnated with TiO_2 as a potential adsorbent for removal of As(III) from water, Catalysts 10 (2020) 1–18, https://doi.org/10.3390/catal10101125.

[27] B.R. Poudel, R.L. Aryal, L.B. Khadka, K.N. Ghimire, H. Paudyal, M.R. Pokhrel, Development of biomass-based anion exchanger for the removal of trace concentration of phosphate from water, J. Nepal Chem. Soc. 41 (1) (2020) 56–63.

[28] A. Bingol, H. Ucun, Y.K. Bayhan, A. Karagunduz, A. Cakici, B. Keskinler, Removal of chromate anions from aqueous stream by a cationic surfactant-modified yeast, Bioresour. Technol. 94 (2004) 245–249, https://doi.org/10.1016/j.biortech.2004.01.018.

[29] A. Shrestha, B.R. Poudel, M. Silwal, M.R. Pokhrel, Adsorptive removal of phosphate onto iron loaded *Litchi chinensis* seed waste, J. Instr. Sci. Technol. 23 (2019) 81–87, https://doi.org/10.3126/jist.v23i1.22200.

[30] P. Atreya, C. Shrestha, B. Suvedi, S. Pandey, Emerging fruits of Nepal: pomegranate, kiwifruit, avocado, dragon fruit and grape; opportunities, challenges and ways forward. Presented at Proceeding of 11th National Horticulture Seminar 2020, Kritipur, Kathmandu, February 6-7, 10.

[31] N. Bellahsen, G. Varga, N. Halyag, S. Kertész, E. Tombácz, C. Hodúr, Pomegranate peel as a new low-cost adsorbent for ammonium removal, Int. J. Environ. Sci. Technol. 18 (2021) 711–722, https://doi.org/10.1007/s13762-020-02863-1.

[32] P.L. Homagai, K.N. Ghimire, K. Inoue, Adsorption behavior of heavy metals onto chemically modified sugarcane bagasse, Bioresour. Technol. 101 (2010) 2067–2069, https://doi.org/10.1016/j.biortech.2009.11.073.

[33] M. Ioelovich, Study of cellulose interaction with concentrated solutions of sulfuric acid, ISRN Chem. Eng. (2012) 1–7, https://doi.org/10.5402/2012/428974.

[34] B.H. Hameed, A.A. Ahmad, Batch adsorption of methylene blue from aqueous solution by garlic peel, an agricultural waste biomass, J. Hazard Mater. 164 (2009) 870–875, https://doi.org/10.1016/J.JHAZMAT.2008.08.084.

[35] H. Ucun, Y.K. Bayhan, Y. Kaya, A. Cakici, O.F. Algur, Biosorption of lead (II) from aqueous solution by cone biomass of *Pinus sylvestris*, Desalination 154 (2003) 233–238, https://doi.org/10.1016/S0011-9164(03)80038-3.

[36] I. Langmuir, The constitution and fundamental properties of solids and liquids, J. Am. Chem. Soc. 38 (1916) 2221–2295.

[37] H. Freundlich, About adsorption in solutions, J. Phys. Chem. 57 (1) (1907) 385–470.

[38] M.A. Al-Ghouti, D.A. Da'ana, Guidelines for the use and interpretation of adsorption isotherm models: a review, J. Hazard Mater. 393 (2020), 122383, https://doi.org/10.1016/j.jhazmat.2020.122383.

[39] Lagergren, Zur theorie der sogenannten adsorption geloster stoffe. Kungliga svenska vetenskapsakademiens, Handlingar 24 (1998) 1–39.

[40] Y.S. Ho, Review of second-order models for adsorption systems, J. Hazard Mater. 136 (2006) 681–689, https://doi.org/10.1016/J.JHAZMAT.2005.12.043.

[41] W.J. Weber, J.C. Morris, Kinetics of adsorption carbon from solution, J. Sanit. Eng. Div. 89 (2) (1963) 31–59.

[42] R.A.K. Rao, F. Rehman, Adsorption studies on fruits of Gular (*Ficus glomerata*): removal of Cr(VI) from synthetic wastewater, J. Hazard Mater. 181 (2010) 405–412, https://doi.org/10.1016/J.JHAZMAT.2010.05.025.

[43] L. Xu, Y. Liu, J. Wang, Y. Tang, Z. Zhang, Selective adsorption of Pb^{2+} and Cu^{2+} on amino-modified attapulgite: kinetic, thermal dynamic and DFT studies, J. Hazard Mater. 404 (2021), 124140, https://doi.org/10.1016/j.jhazmat.2020.124140.

[44] X. Zhou, X. Zhou, The unit problem in the thermodynamic calculation of adsorption using the Langmuir Equation, Chem. Eng. Commun. 201 (2014) 1459–1467, https://doi.org/10.1080/00986445.2013.818541.

[45] H. Paudyal, K. Ohto, H. Kawakita, K. Inoue, Recovery of fluoride from water through adsorption using orange-waste gel, followed by desorption using saturated lime water, J. Mater. Cycles Waste Manag. 22 (2020) 1484–1491, https://doi.org/10.1007/s10163-020-01042-1.

[46] B.R. Poudel, R.L. Aryal, S.K. Gautam, K.N. Ghimire, H. Paudyal, M.R. Pokhrel, Effective remediation of arsenate from contaminated water by zirconium modified pomegranate peel as an anion exchanger, J. Environ. Chem. Eng. 9 (2021), 106552, https://doi.org/10.1016/j.jece.2021.106552.

[47] R. Labied, O. Benturki, A.Y. Eddine Hamitouche, A. Donnot, Adsorption of hexavalent chromium by activated carbon obtained from a waste lignocellulosic material (Ziziphus jujuba cores): kinetic, equilibrium, and thermodynamic study, Adsorpt. Sci. Technol. 36 (2018) 1066–1099, https://doi.org/10.1177/0263617417750739.

[48] R. Chakraborty, R. Verma, A. Asthana, S.S. Vidya, A.K. Singh, Adsorption of hazardous chromium (VI) ions from aqueous solutions using modified sawdust: kinetics, isotherm and thermodynamic modelling, Int. J. Environ. Anal. Chem. 101 (2021) 911–928, https://doi.org/10.1080/03067319.2019.1673743.

[49] C. Namasivayam, M.V. Sureshkumar, Removal of chromium(VI) from water and wastewater using surfactant modified coconut coir pith as a biosorbent, Bioresour. Technol. 99 (2008) 2218–2225, https://doi.org/10.1016/j.biortech.2007.05.023.

[50] Q. Wang, C. Zhou, Y. jie Kuang, Z. hui Jiang, M. Yang, Removal of hexavalent chromium in aquatic solutions by pomelo peel, Water Sci. Eng. 13 (2020) 65–73, https://doi.org/10.1016/j.wse.2019.12.011.

[51] A.S. Santos, T.S.M. Santos, V.A. Lemos, Yellow mombin (*Spondias mombin L.*) seeds from agro-industrial waste as a novel adsorbent for removal of hexavalent chromium from aqueous solution, J. Braz. Chem. Soc. 32 (2) (2021) 437–446.

[52] R. Chand, K. Narimura, H. Kawakita, K. Ohto, T. Watari, K. Inoue, Grape waste as a biosorbent for removing Cr(VI) from aqueous solution, J. Hazard Mater. 163 (2009) 245–250, https://doi.org/10.1016/j.jhazmat.2008.06.084.

[53] J.W. Ball, D.K. Nordstrom, Critical evaluation and selection of standard state thermodynamic properties for chromium metal and its aqueous ions, hydrolysis species, oxides, and hydroxides, J. Chem. Eng. Data 43 (1998) 895–918, https://doi.org/10.1021/je980080a.
[54] C. Balan, I. Volf, D. Bilba, Uklanjanje hroma (VI) iz vodenih rastvora pomoću purolita - Bazne anjonske smole sa gel strukturom, Chem. Ind. Chem. Eng. Q. 19 (2013) 615–628, https://doi.org/10.2298/CICEQ120531095B.
[55] A. Nakajima, Y. Baba, Mechanism of hexavalent chromium adsorption by persimmon tannin gel, Water Res. 38 (2004) 2859–2864, https://doi.org/10.1016/j.watres.2004.04.005.
[56] S.G. Prabhu, G. Srinikethan, S. Hegde, Pelletization of pristine Pteris vittata L. pinnae powder and its application as a biosorbent of Cd(II) and Cr(VI), SN Appl. Sci. 2 (2020) 1–9, https://doi.org/10.1007/s42452-019-1906-1.
[57] A. Pholosi, E.B. Naidoo, A.E. Ofomaja, Intraparticle diffusion of Cr(VI) through biomass and magnetite coated biomass: a comparative kinetic and diffusion study, South Afr. J. Chem. Eng. 32 (2020) 39–55, https://doi.org/10.1016/j.sajce.2020.01.005.
[58] A.L. Cazetta, A.M.M. Vargas, E.M. Nogami, M.H. Kunita, M.R. Guilherme, A.C. Martins, T.L. Silva, J.C.G. Moraes, V.C. Almeida, NaOH-activated carbon of high surface area produced from coconut shell : kinetics and equilibrium studies from the methylene blue adsorption, Chem. Eng. J. 174 (2011) 117–125, https://doi.org/10.1016/j.cej.2011.08.058.
[59] S. Norouzi, M. Heidari, V. Alipour, O. Rahmanian, M. Fazlzadeh, F. Mohammadi-moghadam, H. Nourmoradi, B. Goudarzi, K. Dindarloo, Preparation, characterization and Cr(VI) adsorption evaluation of NaOH-activated carbon produced from Date Press Cake; an agro-industrial waste, Bioresour. Technol. 258 (2018) 48–56, https://doi.org/10.1016/J.BIORTECH.2018.02.106.
[60] X. Dong, L.Q. Ma, Y. Li, Characteristics and mechanisms of hexavalent chromium removal by biochar from sugar beet tailing, J. Hazard Mater. 190 (2011) 909–915, https://doi.org/10.1016/j.jhazmat.2011.04.008.
[61] M. Chiban, G. Carja, G. Lehutu, F. Sinan, Equilibrium and thermodynamic studies for the removal of As(V) ions from aqueous solution using dried plants as adsorbents, Arab. J. Chem. 9 (2016) S988–S999, https://doi.org/10.1016/j.arabjc.2011.10.002.
[62] S. Lata, P.K. Singh, S.R. Samadder, Regeneration of adsorbents and recovery of heavy metals: a review, Int. J. Environ. Sci. Technol. 12 (2015) 1461–1478, https://doi.org/10.1007/s13762-014-0714-9.
[63] H. Ma, J. Yang, X. Gao, Z. Liu, X. Liu, Z. Xu, Removal of chromium (VI) from water by porous carbon derived from corn straw: Influencing factors, regeneration and mechanism, J. Hazard Mater. 369 (2019) 550–560, https://doi.org/10.1016/j.jhazmat.2019.02.063.
[64] Z. Ye, X. Yin, L. Chen, X. He, Z. Lin, C. Liu, S. Ning, X. Wang, Y. Wei, An integrated process for removal and recovery of Cr(VI) from electroplating wastewater by ion exchange and reduction–precipitation based on a silica-supported pyridine resin, J. Clean. Prod. 236 (2019), 117631, https://doi.org/10.1016/J.JCLEPRO.2019.117631.
[65] S. Nag, N. Bar, S.K. Das, Cr(VI) removal from aqueous solution using green adsorbents in continuous bed column – statistical and GA-ANN hybrid modelling, Chem. Eng. Sci. 226 (2020), 115904, https://doi.org/10.1016/J.CES.2020.115904.
[66] S. Pourfadakari, S. Jorfi, M. Ahmadi, A. Takdastan, Experimental data on adsorption of Cr(VI) from aqueous solution using nanosized cellulose fibers obtained from rice husk, Data Brief 15 (2017) 887–895, https://doi.org/10.1016/j.dib.2017.10.043.